SPANDIDOS PUBLICATIONS

ONCOLOGY LETTERS 28: 468, 2024

Myeloid/lymphoid neoplasms with eosinophilia and FGFR1 rearrangement t(8;13)(p11;q12): A case report and literature review

YU-JIE GUO, MENG-XUE MA, TIAN TIAN, JING-NAN ZHANG, XIAO-NAN GUO and SHUKAI QIAO

Department of Hematology, The Second Hospital of Hebei Medical University, Shijiazhuang, Hebei 050000, P.R. China

Received March 4, 2024; Accepted June 25, 2024

DOI: 10.3892/ol.2024.14601

Abstract. 8p11 myeloproliferative syndrome (EMS) is a rare and aggressive hematological malignancy, characterized by myeloproliferative neoplasms, and associated with eosinophilia and T- or B-cell lineage lymphoblastic lymphoma. The pathogenesis is defined by the presence of chromosomal translocations associated with the fibroblast growth factor-1 (*FGFR1*) gene, located in the 8p11-12.1 chromosomal locus. At present, only ~100 cases have been reported globally. At least 15 partner genes have been identified, including the most common, the zinc finger MYM-type containing 2 (*ZNF198)-FGFR1* fusion gene formed by t(8;13)(p11;q12). Different fusion genes determine the clinical manifestations and prognosis of the disease. Patients with EMS with t(8;13)(p11;q12) commonly present with lymphadenopathy and T-lymphoblastic lymphoma, which usually converts to acute myeloid leukemia (AML) with the progression of the disease. The present study describes the case of an elderly female patient with EMS with t(8;13)(p11;q12), presenting with myeloid/lymphoid syndrome (myeloproliferative neoplasms and T lymphoblastic lymphoma). The patient received the CHOPE regimen combined with tyrosine kinase inhibitor (dasatin) treatment and obtained short-term complete remission. However, 6 months later, the disease progressed from EMS to AML and the patient died due to ineffective induction therapy. The present study also reviews the relevant literature about this unusual entity to enhance the understanding of EMS.

Introduction

8p11 myeloproliferative syndrome (EMS), first reported by Macdonald *et al* (1) in 1995, is a rare atypical myeloproliferative disease, and is also termed stem cell leukemia/lymphoma syndrome. The disease is characterized by a significantly higher peripheral white blood cell count (WBC), myeloid cell hyperplasia and eosinophilia in the bone marrow, lymph node pathology for lymphoblastic lymphoma and involvement of the short arm of chromosome 8 (8p11) for fibroblast growth factor-1 (*FGFR1*) gene translocation. Furthermore, EMS can progress to acute leukemia in the short term (2-4). The World Health Organization (WHO) designated EMS for myeloid/lymphoid neoplasms with FGFR1 rearrangement (MLNAF) in 2008. The designation was maintained in the fourth edition of the WHO classification of hematopoietic and lymphoid tissue tumors revised in 2016 (5).

Globally, there have been only ~100 cases of MLNAF reported to date. In 1992, Abruzzo *et al* (6), for the first time, reported the cases of 3 patients with T lymphoblastic lymphoma and peripheral blood eosinophilia. All patients subsequently developed myeloid malignancy, and were gradually diagnosed with EMS. The occurrence of MLNAF is closely associated with *FGFR1* gene abnormalities. *FGFR1* encodes a receptor tyrosine kinase transmembrane protein and belongs to the FGFR family. Under normal conditions, *FGFR1* exists in the form of an oligomer, which binds to its ligand and induces homologous dimerization and self-phosphorylation of *FGFR1*, thereby activating multiple effectors and producing signals for proliferation and survival (7). *FGFR1* gene abnormalities in patients with MLNAF often manifest as translocation or insertion mutations, with gene translocation being the most common. At present, 15 partner genes have been identified for MLNAF, including *ZNF198 (13p12), BCR (22q11), CEP110 (9q33), FGFR1OP2 (12p11), FOP (6q27), TRIM24 (7q34), HERVK (19q13), MYO18A (17q11), NUP98 (11p15), CPSF6 (12p11), CUX1 (7q22), RANBP2 (2q12), TPR (1q25), SQSTM 1 (5q35)* and *LRRFIPI (2q37)* (3,8). In addition, two types of insertion changes, insertion (13;8)(q12;p11p23) and insertion (12;8)(p11;p11;p22) (9,10) have been observed. At present, no gene amplification or deletion mutations have been reported. The products formed by balanced translocation or insertion after *FGR1* gene break exhibit ligand independent *FGFR1* tyrosine kinase activity, and multiple downstream signaling pathways, including the Ras/mitogen-activated protein kinase (Ras/MAPK), phosphatidylinositol 3-kinase (PI3K), phospholipase C (PLC) 7 and signal transducer and activator of transcription (STAT) pathways, are continuously activated, leading to the development of MLNAF (11).

Correspondence to: Dr Shukai Qiao, Department of Hematology, The Second Hospital of Hebei Medical University, 215 Heping Western Road, Shijiazhuang, Hebei 050000, P.R. China
E-mail: qiaoshukai@hebmu.edu.cn

Key words: 8p11 myeloproliferative syndrome, t(8;13)(p11;q12), T lymphoblastic lymphoma, acute myeloid leukemia, tyrosine kinase inhibitor

Few cases concerning MLNAF with t(8;13)(p11;q12) have been reported in the literature, and the outcome of most cases of EMS is poor, even in patients that have been treated with allogeneic stem cell transplantation. In the present study, the case of a patient with MLNAF with t(8;13)(p11;q12) who was treated with a tyrosine kinase inhibitor (TKI) combined with chemotherapy was reported. The aim of the present study is to improve the understanding of EMS.

Case report

A 62-year-old female with no history of hematological disease was admitted to the Department of Hematology, The Second Hospital of Hebei Medical University (Shijiazhuang, China) in November 2019 due to a painless groin mass that had been present for >2 months and a repeating recurrent rash lasting for 1 month. The patient had a history of an elevated peripheral leukocyte level, first reported 11 months prior (range, 11.1-61.8x10^9/l; normal range, 3.5-9.5x10^9/l), which was left untreated. Physical examination revealed extensive red papules and maculopapules on the skin, as well as enlarged lymph nodes in the neck, armpits and groin. The largest lymph node was located in the right groin, measuring ~4x4 cm, with a hard texture and no tenderness. The liver palpation indicated a protrusion of ~1 cm below the costal margin, while the splenic palpation discerned an extension of ~6 cm below the costal margin. The palpitations were homogeneous and had no tenderness.

At admission, the initial peripheral blood analysis revealed a WBC of 136.9x10^9/l (normal range, 3.5-9.5x10^9/l), with neutrophils accounting for 93.06% (normal range, 40-75%) and eosinophils for 0.97% (normal range, 0.4-8%), a hemoglobin level of 151 g/l (normal range, 115-150 g/l) and a platelet count of 208x10^9/l (normal range, 125-350x10^9/l). The eosinophil count, several serum analysis results and eosinophil percentages in the bone marrow at different stages of diagnosis, remission, relapse and AML transformation are summarized in Table I. The bone marrow was hypercellular, with an increased percentage of granules associated with eosinophilia, thus indicating that the patient did not have chronic myeloid leukemia (Fig. 1).

Analyses of the breakpoint cluster region-abelson leukemia virus (*BCR-ABL)* fusion gene, Janus kinase 2 *(JAK2)-V617F*, calreticulin (*CALR)* and myeloproliferative leukemia virus oncogene (*MPL)* mutations, and the next-generation sequencing of gene mutations related to myeloid tumors all gave negative results. The *BCR-ABL* fusion gene testing process was as follows: First, 0.8% ammonium chloride red blood cell lysate was added to the bone marrow fluid and centrifuged at 1,000 x g for 10 min at room temperature to obtain white blood cells. RNA was extracted using the RNA pred Pure Hi-Blood kit (Tiangen Biotech Co., Ltd.; cat. no. DP443), according to the manufacturer's instructions. A total of 1 ml Trizol was added to a 50-μl leukocyte suspension and mixed. The solution was incubated at room temperature for 5 min, followed by the addition of 0.2% chloroform. After shaking for 30 sec, it was left undisturbed for 3 min and further centrifuged at 16,000 x g for 15 min at 4˚C. The supernatant was transferred into a diethylpyrocarbonatetreated EP tube and mixed with isopropyl alcohol, and left at room temperature for 10 min. RNA was obtained by centrifugation again at 16,000 x g for 5 min at 4˚C. RNA amplification was performed using the BCR-ABL fusion gene detection kit (Bio-Rad Laboratories, Inc.; cat. no. 171V37145) in strict accordance with the instructions provided. The LightCycler 480 fluorescence detector (Roche Diagnostics) was used, and the amplification conditions included a temperature of 42˚C for 30 min, 94˚C for 5 min and 40 cycles. Fluorescence signals were collected at 60˚C during the second step of the PCR cycle, and data analysis software Opticon Monitor realtime v2.02 (Bio-Rad Laboratories, Inc.) was utilized. The JAK2V617F, MPL and CALR testing process was as follows: First, 0.8% ammonium chloride red blood cell lysate was added into the bone marrow fluid and centrifuged at 1,000 x g for 10 min at room temperature to obtain white blood cells. The Tianamp genomic DNA kit (Tiangen Biotech Co., Ltd.; cat. no. DP304) was used to extract intracellular DNA in strict accordance with the instructions provided by the kit. A total of ~20 μl white blood cells and 18 μl protease were mixed well. After which, 200 μl buffer solution was added and the mixture was heated at 70˚C for 10 min. A total of 200 μl anhydrous ethanol was added to the mixture, mixed until white flocculent appeared and then transferred to the centrifugal column. The sample was centrifuged at 13,400 x g for 1 min at room temperature and the waste liquid was discarded from the collection pipe. A total of 500 μl GD was added to the centrifugal column, and the sample was centrifuged at room temperature for 1 min at 13,400 x g. The waste liquid was discarded again and 500 μl bleach solution per wash was added to the centrifugal column, and centrifuged at room temperature for 1 min at 13,400 x g. The waste liquid was discarded once more and centrifuged at 13,400 x g for two min at room temperature. The centrifugal column was placed into a new EP tube, 200 μl TE solution was added and at room temperature centrifuged for 2 min at 13,400 x g in order to obtain DNA. The mutations of JAK2V617F (Exon12), CALR (Exon9) and MPL (Exon10) were qualitatively detected using the ipsogen JAK2 RGQ PCR Kit, ipsogen MPL W515L/K MutaScreen Kit and CALR RGQ PCR Kit (Qiagen AB; cat. nos. 673633, 676413 and 674013, respectively) The instructions of the kit were strictly followed, and ABI PRISM fluorescent PCR detector was used for detection. Amplification conditions included 40 cycles at 42˚C for 5 min and 94˚C for 3 min, and fluorescencemyoproliferative tumor-related gene mutation detection kit signals were collected at 60˚C in the second step of the PCR cycle. The analysis software used was Opticon Monitor realtime v2.02 (Bio-Rad Laboratories, Inc.). The extraction steps of DNA and RNA in next-generation sequencing were as aforementioned. The DNA and RNA were extracted by commercial kits (Tiangen Biotech, Co., Ltd.; cat. nos. is DP340, DP304 and DP431). The purities and concentrations of DNA and RNA were confirmed by Nanodrop 2000 (Thermo Scientific Scientific, Inc.) and Qubit 3.0 Fluorometer (Thermo Fisher Scientific, Inc.). The Qsep400 nucleic acid fragment analyzer (Hangzhou Houze Bio-Technology Co., Ltd.,) was utilized to evaluate the integrity of DNA and RNA. The DNA were transformed into libraries using KAPA EvoPlus Kits (Kapa Biosystems; Roche Diagnostics; cat. no. 9420053001). The libraries were analyzed on the Illumina sequencing platform NextSeq550 using 150-bp paired-end sequencing. Sequencing

Table I. Summary of the eosinophil count, serum analysis results and eosinophil percentages in bone marrow at different stages.

Date	WBCs, n ($x10^9$/l)	Es, %	Es, n ($x10^9$/l)	Hb, g/l	PLTs, n ($x10^9$/l)	LDH (U/l)	B2M (mg/l)	BM (E%)
November 2020-Diagnosis	136.9	0.97	1.33	151	208	588	3.9	9.5
April 2021-Remission	9.6	3.8	0.4	100	200	253	2.9	2
Early July 2021-Relapse	29.1	3.1	0.9	106	276	634	2.9	11
Late July 2021-AML transformation	36.3	0.8	0.3	96	45	1,219	4.3	8

AML, acute myeloid leukemia; WBC, white blood cell; E, eosinophil; PLT, platelet; Hb, hemoglobin; LDH, lactate dehydrogenase; B2M, β2-microglobulin; BM, bone marrow; Es%, percentage of eosinophils.

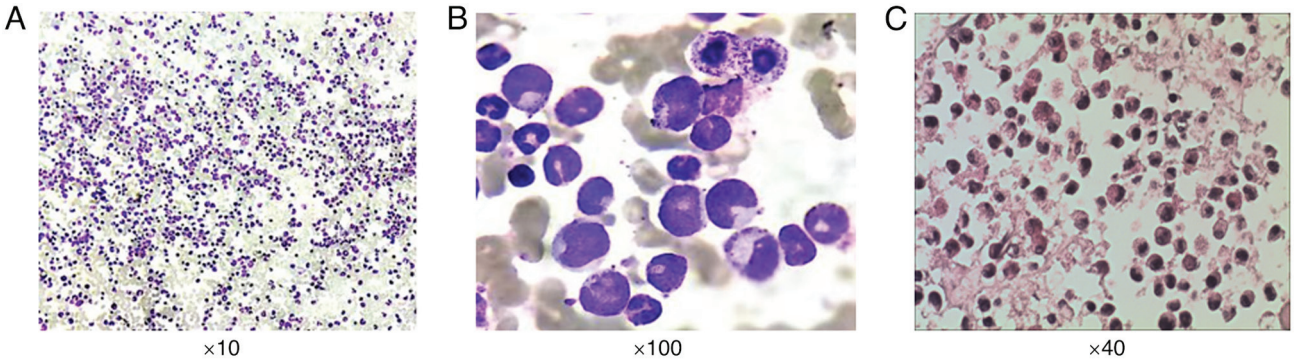

Figure 1. Representative images of bone marrow smear and biopsy. Bone marrow smears at (A) x10 and (B) x100 magnification (Wright-Giemsa stain) showing a myeloproliferative neoplasm with increased numbers of immature myeloid cells and inhibition of erythroid and megakaryocyte proliferation. (C) Bone marrow biopsy showing active bone marrow proliferation (magnification, x40).

was performed using the NextSeq 500/550 High output kit v2.5 (300 cycles; cat. no. 20024908; Illumina Inc). To quantify the final library concentration, the Qubit 3.0 Fluorometer was employed. The loading concentration of the final library was ~14 pM.

Fluorescence *in situ* hybridization (FISH) analysis of the bone marrow showed positive *FGFR1* gene rearrangement (positive rate, 94%), with negative platelet-derived growth factor receptor A (*PDGFRA*) and *PDGFRB* gene rearrangements (Fig. 2). The preparation of the peripheral bone marrow samples from patients for FGFR1, PDGFRA,PDGFRB FISH detection was performed as follows: Initially, the samples were fixed in a fixed solution consisting of methanol to acetic acid (3:1), one pre-fixation step was performed using a 10% fixed solution, and the sample was fixed three times. Next, the fixed cells were placed onto a glass slide to create a sample slide, allowed to air dry, the fragments were washed with 2X saline sodium citrate buffer solution at 37˚C for 30 min, and dehydrated sequentially in 75, 85 and 100% alcohol for 1 min each. The FISH probes FGFR1/D8Z2 (Anbiping; cat. no. F.01109-01), PDGFRA (Anbiping; cat. no. F.01162-01) and PDGFRB (Anbiping; cat. no. F.01033-01) were utilized with a hybridization instrument (Thermos; cat. no. S500-24) for hybridization, denaturing at 78˚C for 8 min, and hybridizing at 42˚C for 16 h. On the following day, the samples were washed with 0.3% NP40 wash solution at 68˚C for 2 min, followed by washing with deionized water at 37˚C for 1 min. DAPI nuclear staining was performed for 20 min at room temperature, and the results were observed using a fluorescence microscope (Olympus; cat. no. BX63). Metasystem ISIS V5.8.11 (Metasystem Co., Ltd.) FISH analysis software was used for photography and analysis purposes. The karyotype showed a balanced translocation between chromosome 8 and chromosome 13: t(8;13)(p11;q12) (Fig. 3). Positron emission tomography (PET)/computed tomography (CT) scans showed a diffuse increase in bone marrow metabolic activity, multiple high metabolic lymph nodes above and below the diaphragm, and splenomegaly with increased metabolic activity, consistent with the manifestation of lymphoma (Fig. S1).

A right inguinal lymph node biopsy revealed disruption of the normal structure with diffuse infiltration by lymphoblasts. The immunophenotype was as follows: CD3(+), CD5(+), CD43(+), CD99(+), terminal deoxynucleotidyl transferase (partial +), CD34(-), Ki-67(+ 70%), CD20(-), CD21(-), CD56(-), myeloperoxidase(-), CD68 (loose +), BCL-2(-), BCL-6(-), CD10(-), CD117(-), CD15(-), cyclinD1(-), mutated melanoma-associated antigen 1(-), paired box protein Pax-5(-) and Epstein-Barr virus-encoded small RNA(-). In order to further investigate the expression of immature markers in this patient with T lymphoblastic lymphoma, the immunohistochemical staining of CD1A, CD4 and CD8 was also performed. The results indicated that the samples were partially positive for CD1A, positive for CD4 and negative for CD8 (Fig. 4). The lymph nodes were immersed in a 4% formaldehyde solution

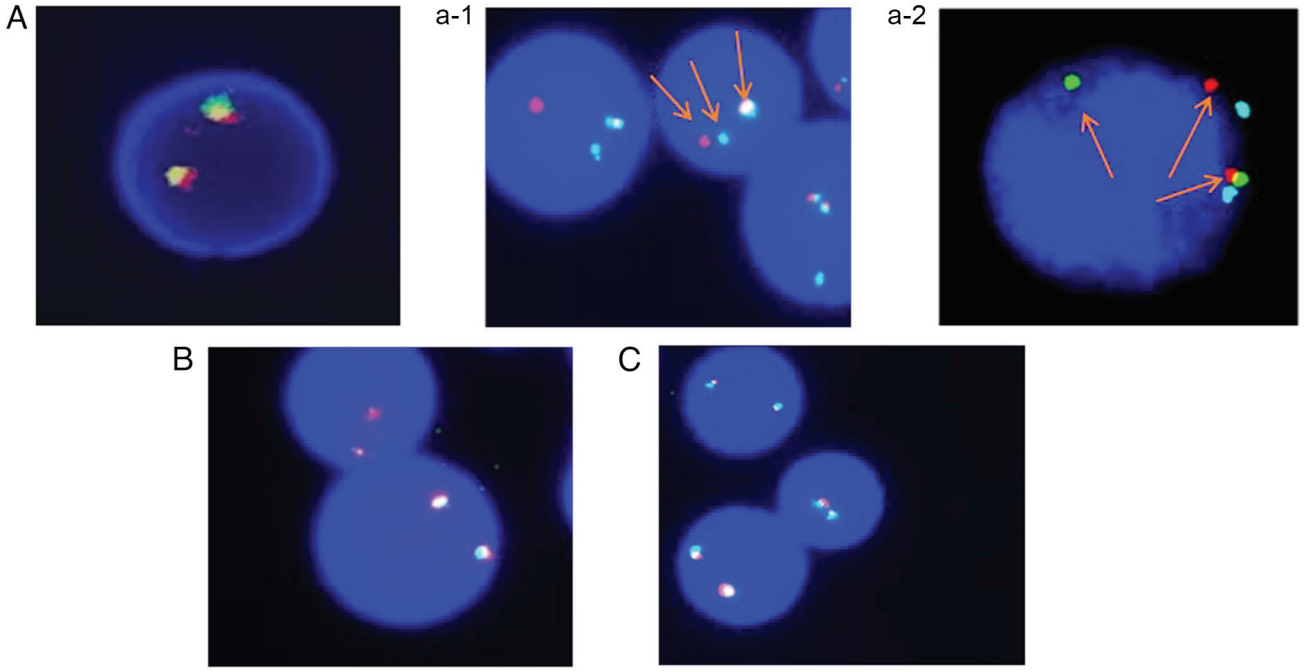

Figure 2. Fluorescence *in situ* hybridization analysis of *FGFR1* gene rearrangement in bone marrow cells. A total of three sets of probes were used to count 200 interphase cells. (A) Normal control of *FGFR1* gene showing a red-green fusion signal; (a-1) *FGFR1* gene showing 1 red, 1 green and 1 fusion signal, confirming the presence of the pre-treatment FGFR1 (8p11) gene rearrangement. (a-2) The FGFR1 gene showed 1 red, 1 green and 1 fusion signal, indicating that FGFR1 (8p11) gene rearrangement had not disappeared after treatment. (B) *PDGFRA* gene showing a red-green and blue fusion signal, and no abnormal signal of the *PDGFRA* gene. (C) *PDGFRB* gene showing a red and green fusion signal, and no abnormal signal of the *PDGFRB* gene. FGFR1, fibroblast growth factor receptor 1; PDGFR, platelet-derived growth factor receptor.

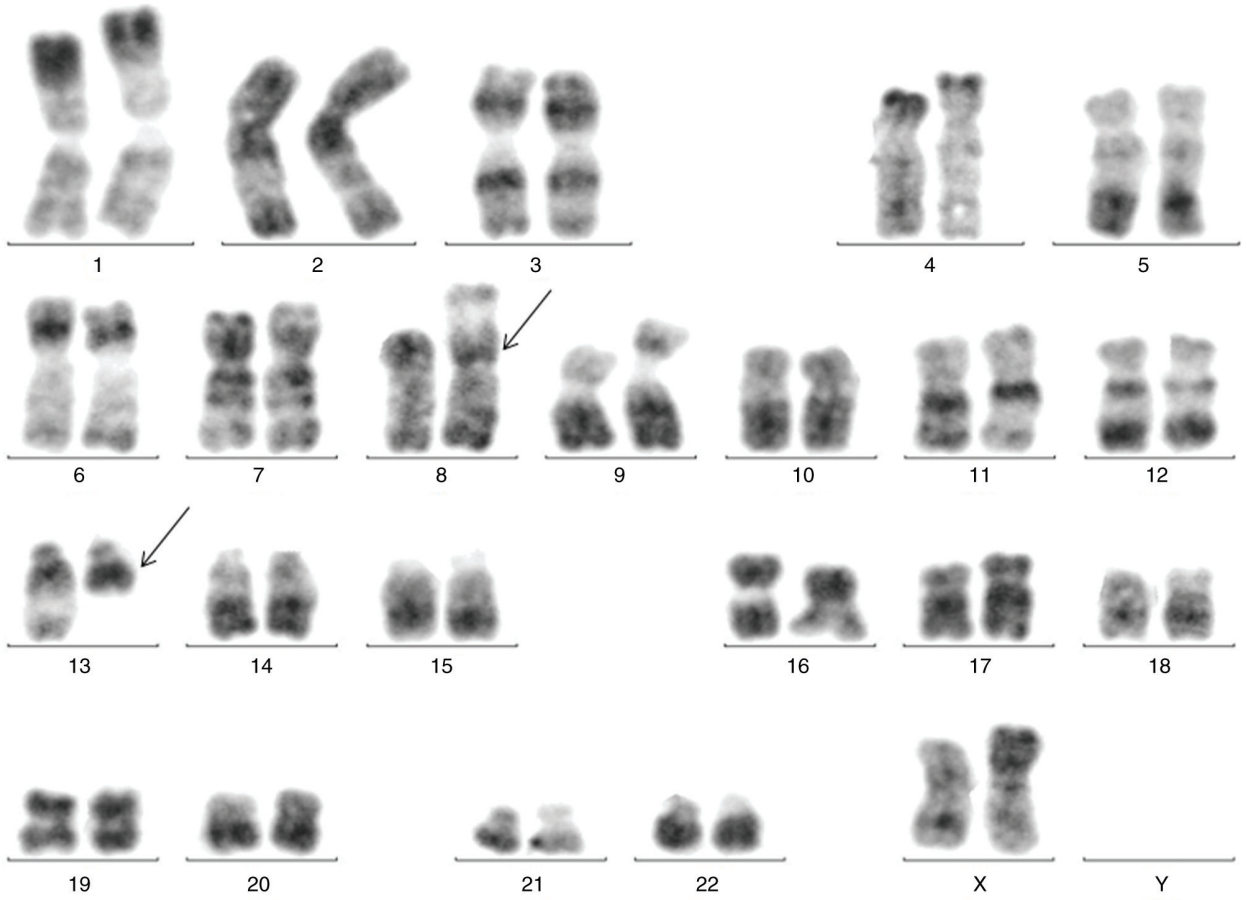

Figure 3. Results of chromosomal karyotype analysis from bone marrow cells. G-banded karyotype of bone marrow cells demonstrating a translocation between chromosome 8p11 and 13q12 (arrows indicate rearranged chromosomes).

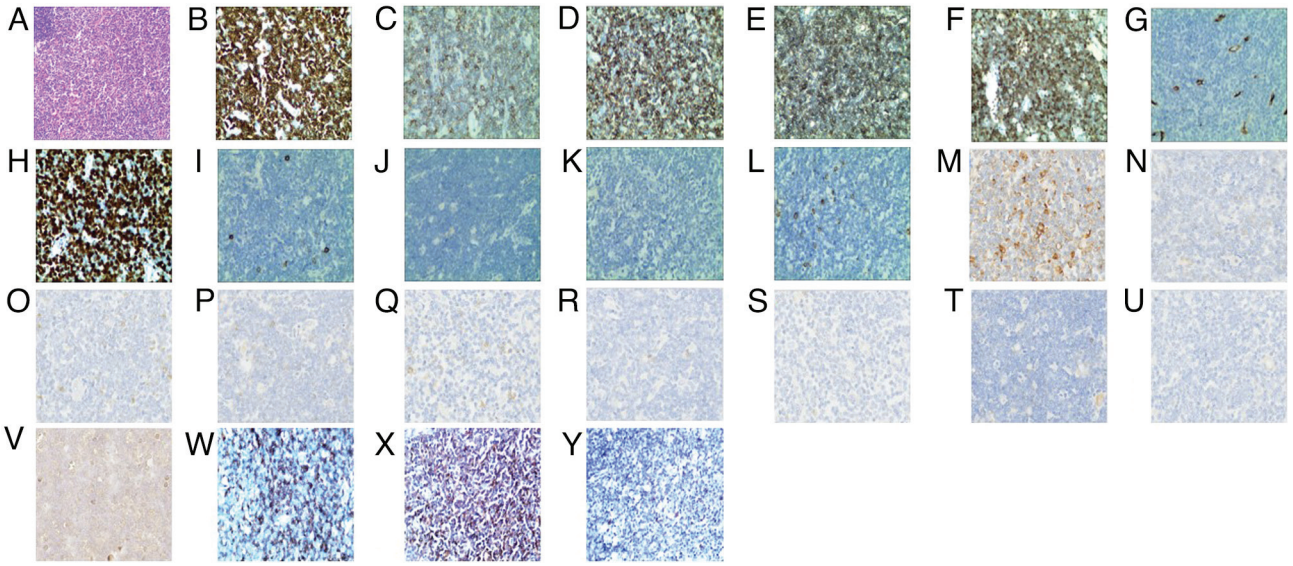

Figure 4. Right inguinal lymph node biopsy with an (A) hematoxylin and eosin-stained section (magnification, 100x) showing partial disappearance of the normal structure. Tumor cells (magnification, 400x) (B) CD3-diffusely bright positive, (C) CD5-positive, (D) CD43-positive, (E) CD99-positive, (F) terminal deoxynucleotidyl transferase partially positive, (G) CD34-negative, (H) diffusely bright Ki-67-positive (+70%), (I) CD20-negative, (J) CD21-negative, (K) CD56-negative, (L) myeloperoxidase-negative, (M) CD68-(loose positive), (N) Bcl-2-negative, (O) Bcl-6-negative, (P) CD10-negative, (Q) CD117-negative, (R) CD15-negative, (S) cyclinD1-negative, (T) MUM-1-negative, (U) PAX-5-negative, (V) EBER-negative, (W) CD1A-positive, (X) CD4-positive and (Y) CD8-negative.

and fixed overnight at 4 ˚C. The following day the tissue was dehydrated and embedded in paraffin wax. The embedded material was cut into 4-μm slices, dewaxed and rehydrated, and the antigens were extracted. The slices were incubated with 3% hydrogen peroxide at room temperature for 4 min. After washing with PBS, they were blocked with 5-10% normal goat serum (cat. no. ab7481; Abcam) in PBS, incubated at room temperature for 10 min, and the serum was removed. The following primary antibodies were added: Anti-CD1A (cat. no. ab313875; 0.1 μg/ml; Abcam), anti-CD4 (cat. no. ab133616; 0.2 μg/ml; Abcam), anti-CD8 (cat. no. ab245118; 0.4 μg/ml; Abcam), anti-CD3 (cat. no. ab243874; 0.2 μg/ml; Abcam), anti-CD43 (cat. no. ab101533; 0.5 μg/ml; Abcam), anti-CD5 (cat. no. ab75877; 0.2 μg/ml; Abcam), anti-CD68 (cat. no. ab213363; 0.08 μg/ml; Abcam), anti-CD99 (cat. no. ab108297; 0.5 μg/ml; Abcam), anti-terminal deucleotide transferase (cat. no. ab183341; 1 ug/ml; Abcam), anti-Ki-67 (cat. no. ab92742; 1 μg/ml; Abcam), anti-Bcl-2 (cat. no. ab32124; 1 μg/ml; Abcam), anti-Bcl-6 (cat. no. ab172610; 0.5 μg/ml; Abcam), anti-CD10 (cat. no. ab208778; 0.1 μg/ml; Abcam), anti-CD117 (cat. no. ab32363; 1 μg/ml; Abcam), anti-CD15 (cat. no. ab218403; 5 μg/ml; Abcam), anti-CD20 (cat. no. ab219329; 1 μg/ml; Abcam), anti-CD21 (cat. no. ab315160; 2 μg/ml; Abcam), anti-CD34 (cat. no. ab315820; 0.1 μg/ml; Abcam), anti-CD56 (cat. no. ab313779; 0.2 μg/ml; Abcam), anti-cyclind1 (cat. no. ab273608; 1 μg/ml; Abcam), anti-myeloperoxidase (cat. no. ab134142; 0.1 μg/ml; Abcam), anti-mutated melanoma-associated antigen 1 (cat. no. ab247079; 0.5 μg/ml; Abcam), anti-pin-box protein Pax-5 (cat. no. ab234402; 0.5 μg/ml; Abcam) and incubated at 3˚C for 1-2 h or 4˚C overnight. After washing with PBS for three times, biotin-labeled secondary antibody (HRP marker; cat. no. ab6721; 1 μg/ml; Abcam) was added to the working solution and incubated at 37˚C for 20-40 min. The sample was washed with PBS three times, streptavidin coupled alkaline phosphatase was added and incubated at 37˚C for 15-25 min. The sample was rinsed again with PBS and 3,3'-diaminobenzidine was added at room temperature for 3-15 min for color development. Section cleaning, hematoxylin reverse staining, dehydration, cleaning and mounting was performed. *In situ* hybridization was used to detect encoded small RNA (EBER) of Epstein-Barr virus. EBER *in situ* hybridization kit (cat. no. ISH 7001) from ZSBG-Bio was used. The dewaxed and hydrated lymph node sections were added with 1X protease K working solution and incubated at room temperature for 5 min. After which, EBER hybrid solution was added and incubated at 55˚C for 60 min, and finally transferred to 37˚C for overnight incubation. After washing with PBS, HRP-marked digoxin antibody was added. After incubation at 37˚C for 30 min, DAB color developing solution was added, and hematoxylin was re-stained at room temperature for 1-2 min, dehydrated and sealed. Representative images are taken with a light microscope (Japan). This was consistent with the immunophenotype of typical T lymphoblastic lymphoma. Based on the aforementioned immunohistochemical staining, the biopsy of the right inguinal lymph node was consistent with T lymphoblastic lymphoma. *FGFR1* gene rearrangement was also positive in the right inguinal lymph node tissue sections, as indicated by FISH (Fig. 5). Therefore, a diagnosis of MLNAF with t(8;13)(p11;q12) was made. At that time, the FGFR1 partner gene was not detected. Previously, paraffin-embedded samples of the lymph nodes of patient were used to detect the presence of the FGFR1-ZNF198 fusion gene by reverse transcription polymerase chain reaction quantification (RT-qPCR. The lymph node paraffin-embedded specimen was sliced and placed in a centrifuge tube. The tissue was dewaxed using xylene. RNA was extracted using the RNA pred Pure Hi-Blood kit (Tiangen Biotech Co., Ltd.; cat. no. DP443), in strict accordance with the

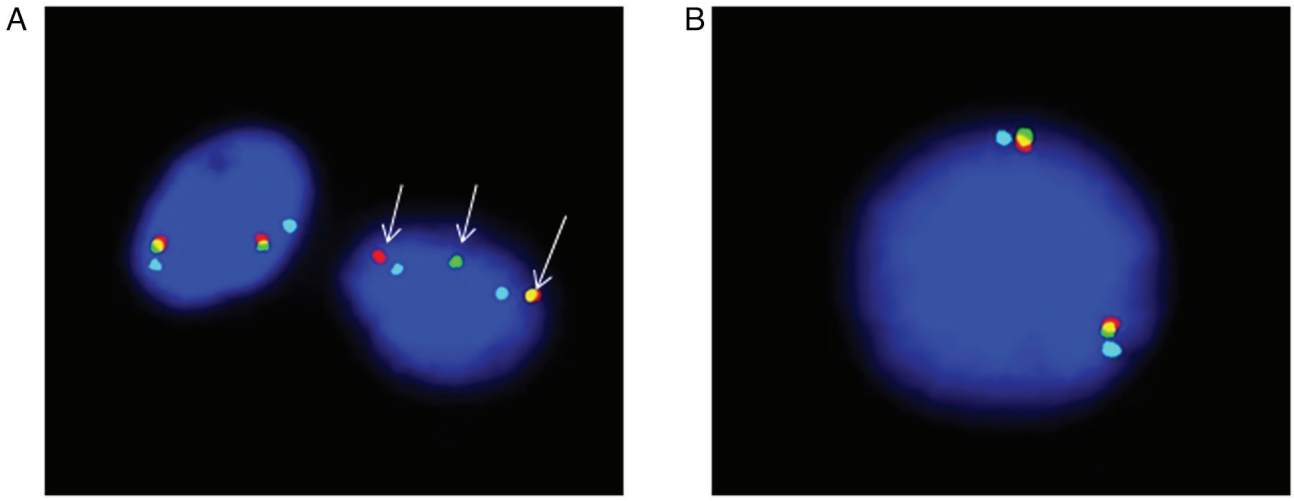

Figure 5. *FGFR1* gene rearrangement confirmed by fluorescence *in situ* hybridization in the right inguinal lymph node section of the patient. Using a three-color separation probe, the blue color is the quality control signal. (A) *FGFR1* gene showing 1 red, 1 green and 1 fusion signal in the presence of the FGFR1 (8p11) gene rearrangement. (B) Normal control for the *FGFR1* gene, showing the red and green fusion signals. *FGFR1*, fibroblast growth factor receptor 1.

kit instructions. A total of 1 ml of Trizol (Invitrogen; Thermo Fisher Scientific, Inc.) was added to $1x10^7$ cell suspension and mixed. The mixture was incubated at room temperature for 5 min, followed by the addition of 0.2% chloroform. After shaking for 30 sec, it was left undisturbed for 3 min and then centrifuged at 2-8˚C at 12,000 x g for 15 min. The supernatant was transferred into a DECP-treated EP tube and mixed with isopropyl alcohol, which was left at room temperature for 10 min. RNA was obtained by centrifugation again at 2-8˚C at 12,000 x g for 5 min. cDNA was synthesized from 2 μg total RNA using a first-strand cDNA synthesis kit (cat. no. K1622; Thermo Fisher Scientific, Inc.). The PCR primers of the *FGFR1-ZNF198* fusion gene and normalization control β-actin gene were designed based on the corresponding gene structure using Primer-BLAST (http://www.ncbi.nlm.nih.gov/tools/primer-blast), and the sequences were follows: *FGFR1-ZNF198*, Forward, 5'-TCCCTGTGCCTGTGTATATCCC-3' and reverse, 5'-CGGGAAGCTCATACTCAGAGAC-3'; and β-actin forward, 5'-AAGGCCAACCGCGAGAAGAT-3' and reverse, 5'-TCGGTGAGGATCTTCATGAG-3'. Using SYBR Green (Thermo Fisher Scientific, Inc.) as the fluorophore, the amplification conditions included a temperature of 42˚C for 30 min, 94˚C for 5 min and 40 cycles. The method of quantification was $2^{-\Delta\Delta Cq}$ (Livak and Schmittgen 2001). Due to the prolonged placement of the specimen, the mRNA was severely degraded and could not be effectively reverse transcribed into cDNA, thus the RT-qPCR could not be completed.

The TKI dasatinib in combination with the CHOPE chemotherapy (2 mg/m^2 vindesine on day 1 + 750 mg/m^2 cyclophosphamide on day 1 + 20 mg/m^2 doxorubicin hydrochloride liposome on day 1 + 60 mg/m^2 etoposide on days 1-3 + 1 mg/kg prednisone tablet on days 1-5) was initiated for 1 cycle, every 21 days. After 4 cycles, the enlarged lymph nodes of the patient disappeared, the liver returned to normal and the spleen shrank to 1 cm below the left costal margin. Furthermore, the peripheral blood count returned to normal, and the proportion of *FGFR1* gene rearrangement detected by bone marrow FISH analysis decreased to 36% (Fig. 2). Finally, PET/CT scans showed partial metabolic remission in April 2021 (Fig. 1). The flow cytometry results of the patient's bone marrow at diagnosis and remission are presented in Fig. 6. EDTA anticoagulant marrow blood and the following antibodies were added: CD45 (cat. no. ab40763; Abcam), CD38 (cat. no. ab108403; Abcam), CD117 (cat. no. ab317843; Abcam), CD7 (cat. no. ab109296; Abcam), HLA-DR (cat. no. ab92511; Abcam), CD16 (cat. no. ab223200; Abcam), CD13 (cat. no. ab317440; Abcam), CD33 (cat. no. ab134115; Abcam), CD56 (cat. no. ab220360; Abcam), CD64 (cat. no. ab109449; Abcam), CD11c (cat. no. ab254183; Abcam), CD15 (cat. no. ab241552; Abcam), CD11b (cat. no. ab224805; Abcam), MPO (cat. no. ab208670; Abcam) and CD79a (cat. no. ab133483; Abcam) at 100 μl/each into the tube, shaken, and kept in darkness at room temperature for 20 min. A total of 3% paraformaldehyde was added and incubated in darkness 10 min at room temperature. A total of 1 ml purified water was added and the solution was kept in darkness at room temperature for 10 min after shaking. The solution was centrifuged at 160 x g for 5 min at room temperature and the supernatant was discarded. A total of 2 ml of PBS solution was added, shaken and centrifuged at 160 x g for 5 min at room temperature. The supernatant was discarded and 500 μl PBS was added. Specimens were examined using Flow cytometer (Beckman Coulter, Inc.) after mixing. The detected data was analyzed by Kaluza 2.1.1 software(Beckman Coulter, Inc). The fluorescent dyes were all obtained from Beckman Coulter, Inc, including fluorescein isothiocyanate (FITC), phycoerythrin (PE), peridinin chlorophy II protion (PreCP) and allophycocyanin (APC). The aforementioned reagents and labeling methods were used to detect known positive specimens as positive controls and the negative cell population of the specimen was used as the negative control. However, upon continuation of the regimen for a further two cycles, the disease relapsed and new enlarged lymph nodes were found in the neck, and the spleen notably increased in size. An adjusted treatment regimen, including BCL2 inhibitor (venetoclax, 100 mg on day 1, 200 mg on day 2 and 400 mg on days 3-14) + demethylated agent (75 mg/m^2

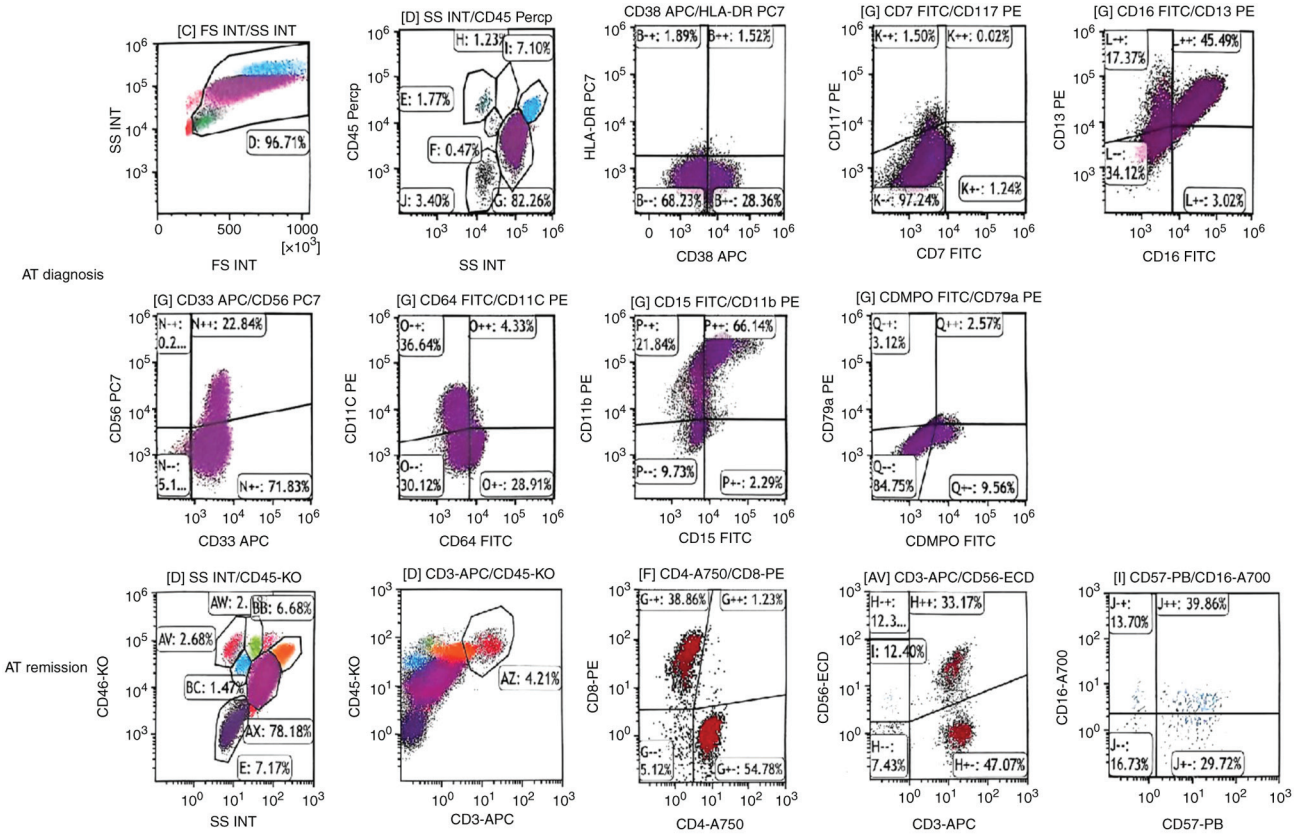

Figure 6. Flow cytometry results of the patient's bone marrow at diagnosis and remission. At diagnosis: The proportion of granulocytes increased, and some cells showed abnormal phenotypic expression. No significant clustering of CD34-positive cells was observed. Most monocytes showed abnormal expression of CD56, while others showed no significant abnormalities. At remission: The ratio of $CD3^+CD4^+/CD3^+CD8^+$ nucleated cells was 1.41, and no abnormal early myeloid cell population was detected.

azacitidine on days 1-7) + histone deacetylase inhibitors (20 mg chidamide twice a week for 2 weeks), was administered. During the treatment process, the WBC count of the patient gradually increased to $60x10^9$/l, and as confirmed by bone marrow cell morphology and flow cytometry, the patient was diagnosed with AML (Fig. 7). The proportion of *FGFR1* gene rearrangement detected by peripheral blood FISH analysis increased to 90%. After diagnosis, the patient was changed to the IA chemotherapy regimen (10 mg/m^2 idarubicin on days 1-3 + 150 mg/m^2 arabinoside on days 1-7) and entered the myelosuppression phase 1 week after chemotherapy. The patient subsequently experienced a severe lung infection and died in August 2021.

Discussion

MLNAF is a malignant tumor originating from hematopoietic stem cells, with various clinical manifestations and aggressive progression; it is slightly more common in men than women, with a median age of 32 years (range, 3-84 years). MLNAF often presents with systemic symptoms such as fatigue, night sweating, emaciation or fever. At initial diagnosis, local or systemic lymph node enlargement and hepatic/splenomegaly are commonly found, and some patients may have extranodal organ involvement, such as that of the tonsils, lungs and mammary glands (3). Approximately one-half of patients with MLNAF possess the t(8;13)(p11;q12) mutation, forming the *ZNF198-FGFR1* fusion gene (3). These patients often show a significant increase in WBC count, and increased eosinophils in the peripheral blood and bone marrow, presenting the coexistence of myeloproliferative neoplasm and T-cell lymphoma. Most of the patients rapidly progress to acute leukemia, commonly AML, within 1-2 years (4). The molecular pathogenesis of MLNAF is characterized by *FGFR1* rearrangement, which forms a fusion gene through translocation, insertion, inversion or deletion (12). This genetic variation impacts *FGFR1* mRNA transcription, thereby promoting the oncogenicity and genetic diversity of the FGFR1 protein. *FGFR1* fusion genes can be divided into two types: Type I and type II. Type I refers to the *FGFR1* gene located at the 3' end of the fusion gene, and the *FGFR1* tyrosine kinase domain is fused to the N-terminal oligomerization domain of the partner protein. This fusion type protein that cannot bind to the FGF ligand and causes a conformational change in the *FGFR1* tyrosine kinase domain. This stimulates the function of *FGFR1* oncogene and constitutively activates its tyrosine kinase function, changes its localization, and subsequently activates PI3K-AKT, RAS/MAPK, STAT and PLC/PKC in the downstream cell pathways to transmit abnormal signals, which ultimately leads to the transition from MLNAF to AML (4,13). The fusion genes of *FGFR1* and its partners in MLNAF belong to type I. Conversely, type II fusion proteins retain the extracellular domain of FGFR1, allowing them to bind to FGF ligands, a characteristic commonly observed in

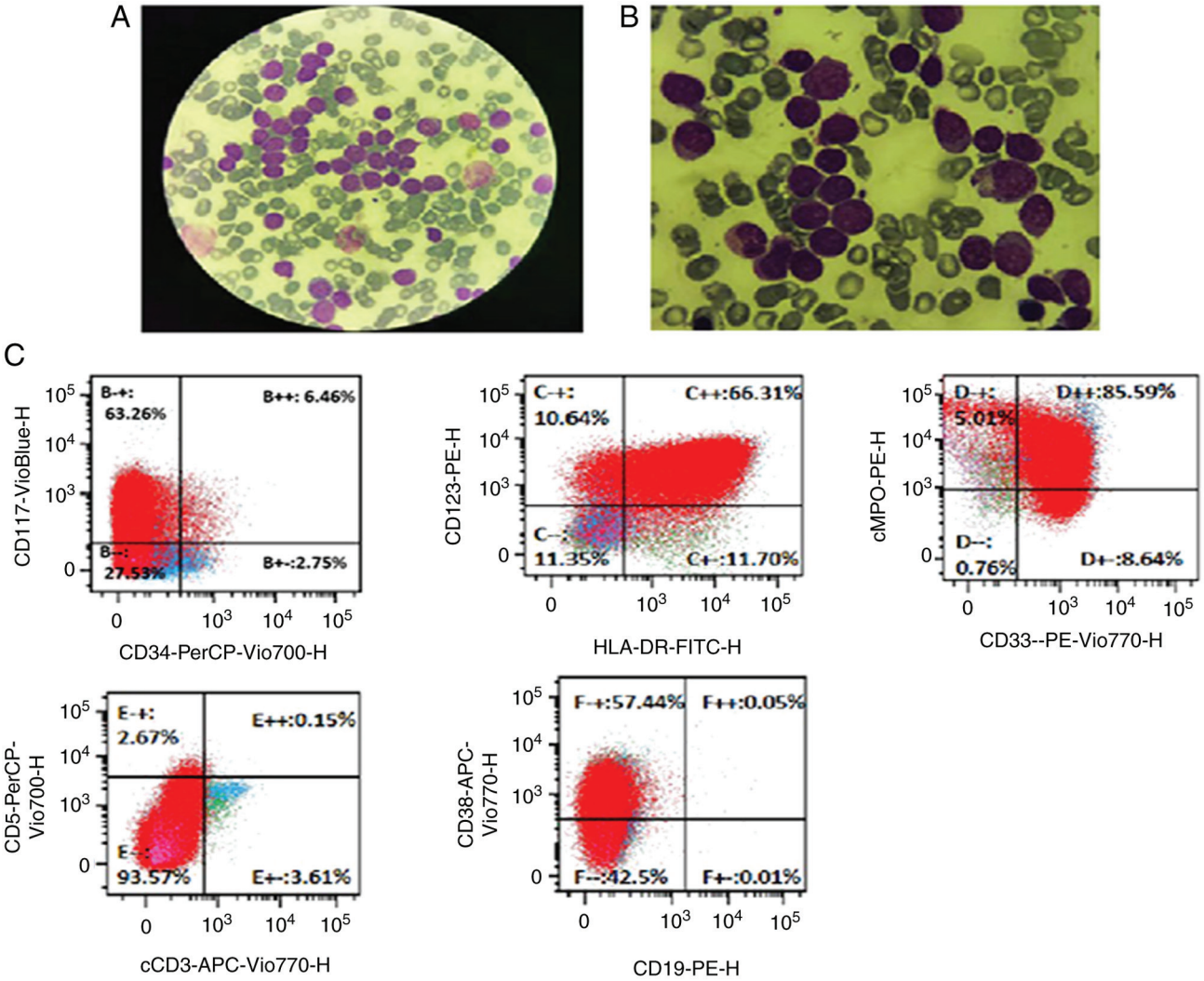

Figure 7. Morphology and flow cytometry analysis of bone marrow aspirate. (A) Bone marrow smear (Giemsa staining) showing significantly increasing myeloid blasts at x10 magnification. (B) Bone marrow smear (Giemsa staining) showing significantly increasing myeloid blasts at x100 magnification. (C) Bone marrow flow cytometry showing AML results: CD117-positive, CD123-positive, HLA-DR-positive, cMPO-positive, CD33-positive; CD5-negative, cCD3-negative and CD19-negative.

solid tumors. Even though the domains in the fusion proteins retained by FGFR rearrangement are different, in all cases the protein retains a complete kinase domain, suggesting that the kinase domain plays a vital role in the function of the fusion protein. The expression of *ZNF198-FGFR1* is related to specific plasminogen activator inhibitor-2-mediated anti-apoptosis, which is possibly one of the reasons for the high malignancy of leukemia cells (14). The numbers and common phenotypes of reported cases for MLNAF, and the reported response for chemotherapy and TKIs have been described in the literature (Table II) (15-36). A review of this literature showed that the cohort of patients with MNLF harboring *ZNF198-FGFR1*, representing the most prevalent cases, predominantly exhibit resistance to chemotherapy (15). While a subset of patients may experience transient responses to TKIs such as imatinib and midostaurin, sustained efficacy remains elusive (16,17). Notably, allogeneic hematopoietic stem cell transplantation was pursued by 9 patients, resulting in remission for 7 patients; however, 2 still experienced disease relapse (4). These findings underscore the insufficiency of traditional chemotherapy and TKIs in addressing this condition.

The patient described in the present study was an elderly woman. The combination of chemotherapy and TKI treatment achieved temporary complete remission; however, the condition rapidly progressed to AML 6 months after the diagnosis, which is consistent with previous literature reports (4,9). At present, there is no unified standard for MLNAF treatment, and conventional cytotoxic drugs have poor therapeutic effects, with the overall survival rate in the literature reportedly <20% (3). FGFR1, as a tyrosine kinase inhibitor receptor, is hypothesized to be a therapeutic target, but neither imatinib nor dasatinib have achieved ideal efficacy. New TKIs, such as pemigatinib and futibatinib, which selectively inhibit FGFR1 tyrosine kinase activity, have shown some efficacy in *in vitro* and animal experiments (37,38), but the exact therapeutic effect still needs to be verified by further clinical trials. Hu *et al* (39) found that the activation of FGFR1 is related to the upregulation of MYC, and there is a synergistic effect between FGFR1 inhibitors and MYC-targeted inhibitors,

Table II. Numbers and common phenotypes of reported cases for myeloid/lymphoid neoplasms with eosinophilia and *FGFR1* rearrangement, and the reported response for chemotherapy and tyrosine kinase inhibitors[a].

Fusion genes	Number of cases	Common phenotypes	Physical and laboratory examination	Sensitivity to chemotherapy	Numbers and results of allo-SCT	Sensitivity to TKIs	(Refs.)
ZNF198-FGFR1	>30	T-LBL/T-lymphoma	Lymphadenopathy, hepatosplenomegaly, eosinophilia or monocytosis or both	Insensitive	7 remission; 2 recurrence	Sensitive (imatinib, midostaurin)	(15-17)
FOP1-FGFR1	5	MPN, AML, B-ALL	Polycythemia without eosinophilia	Sensitive	No	Not tested	(18,19)
CEP110-FGFR1	>20	AML, T-LBL	Lymphadenopathy, purpura, skin lesions, eosinophilia and monocytosis	Insensitive	7 remission; 1 recurrence	Sensitive (imatinib, dasatinib, pemigatinib)	(20,21)
HERVK-FGFR1	2	AML, SM-AHNMD	Polycythemia, poikilocyte, granulocytosis, abnormal megakaryocytes	Insensitive	1 remission	Not tested	(22)
BCR-FGFR1	>30	CML, aCML, AML, B-ALL	Splenomegaly, eosinophilia	Insensitive	4 remission; 3 recurrence	Insensitive (imatinib, dasatinib), Sensitive (ponatinib, pemigatinib)	(23,24)
NUP98-FGFR1	2	Therapeutic AML	Granulocyte hyperplasia with mononucleosis	Not tests	No	Not tested	(25)
FOP2-FGFR1	2	T-LBL, AML	Lymphadenopathy, eosinophilia	Sensitive	No	Not tested	(26)
TIF1-FGFR1	5	CEL, AML	Eosinophilia	Resistant	No	Not tested	(27)
MYO18A-FGFR1	2	CML	Thrombocytopenia, monocyte, eosinophilic and basophil increased	Resistant	No	Not tested	(28)
CPSF6-FGFR1	1	Not reported	Lymphadenopathy and splenomegaly, neutrophils without eosinophilia	Resistant	No	Not tested	(29)
LRRFIP1-FGFR1	1	MDS, AML	Pancytopenia, eosinophilia	Not tests	No	Not tested	(30)

Table II. Continued.

Fusion genes	Number of cases	Common phenotypes	Physical and laboratory examination	Sensitivity to chemotherapy	Numbers and results of allo-SCT	Sensitivity to TKIs	(Refs.)
CUX1-FGFR1	1	Pre-T-LBL	Neutrophils, lymphocytes and monocytes increased without eosinophils	Resistant	No	Not tested	(31)
TPR-FGFR1	4	AML	Lymphadenopathy, increasing monocytes	Insensitive	1 remission	Not tested	(32)
NUP358-FGFR1	2	MDS	Splenomegaly, a little eosinophilia	Sensitive	No	Not tested	(33)
SQSTM1-FGFR1	1	AML	Neutrophils and monocytes increased, megakaryocytes	Not tests	No	Not tested	(34)
TFG-FGFR1	1	AML	Skin ecchymosis and splenomegaly, eosinophilia	Insensitive	No	Resistant (ponatinib)	(35)
HOOK3-FGFR1	1	MDS	Leukocytosis and thrombocytopenia.	Insensitive	No	Resistant (ponatinib)	(36)

[a]The responsiveness to the TKIs and chemotherapy are based on the very few studies that have been reported so far; thus, the data included are not definitive. Additionally, in a number of cases, the TKIs were used in conjunction with other chemotherapies or allo-SCT agents. MPN, myeloproliferative neoplasm; AML, acute myeloid leukemia; CML, chronic myeloid leukemia; MDS, myelodysplastic syndrome; aCML, atypical CML; T-LBL, T lymphoblastic lymphoma; CEL, chronic eosinophilic leukemia; SM-AHNMD, clonal hematological non-mast cell lineage diseases associated with systemic mastocytosis; allo-SCT, allogeneic stem cell transplantation.

suggesting a new approach for MLNAF treatment. Currently, these new targeted drugs are still in the experimental stage, and at present, allogeneic hematopoietic stem cell transplantation (allo-HSCT) is still considered to be the best option for the treatment of MLNAF. A previous case study reported that patients with MLNAF achieved disease-free survival times of up to 16 years when treated with allo-HSCT (40). In addition, another patient with refractory MLNAF received dual umbilical cord blood transplantation and achieved 5 years of disease-free survival (41). In the present study, the patient obtained CR after combination chemotherapy + TKI, and was recommended to receive allo-HSCT. However, due to economic constraints, the patient did not receive the treatment and the disease progressed to AML. Finally, the patient died of a pulmonary infection after induction of remission treatment. The present study further confirms that conventional TKIs combined with chemotherapy have limited efficacy in the treatment of MLNAF, and that allo-HSCT should be performed as early as possible after diagnosis.

In conclusion, MLNAF is a rare malignancy originating from hematopoietic stem cells, which has diverse clinical manifestations and may develop into multiple lineage hematopoietic system tumors. The condition is easily misdiagnosed in the early stage, and diagnostic gold-standard genetic examination reveals *FGFR1* gene breakage and chromosome 8p11 translocation. Conventional TKI chemotherapy has poor efficacy, and new targeted drugs are still under research, which may bring hope for the long-term survival of patients. However, at present, allo-HSCT remains the first choice for MLNAF treatment.

Acknowledgements

Not applicable.

Funding

No funding was received.

Availability of data and materials

The sequencing results and raw data generated in the present study may be found in the BioProject database under accession number PRJNA1120252 or at the following URL: https://www.ncbi.nlm.nih.gov/sra/PRJNA1120252.

Authors' contributions

YG was responsible for clinical data collection, interpretation of the results and drafting the manuscript. SQ participated in the design of the study and provided general support. JZ and XG assisted with the analysis. MM and TT collected important background information, prepared the preliminary work of the manuscript and assisted in preliminary data collection. All authors have read and approved the final version of the manuscript.

Ethics approval and consent to participate

Not applicable.

Patient consent for publication

Written informed consent for publication of the case report, including clinical details and images, was provided by the patient's spouse.

Competing interests

The authors declare that they have no competing interests.

References

1. Macdonald D, Aguiar RC, Mason PJ, Goldman JM and Cross NC: A new myeloproliferative disorder associated with chromosomal translocations involving 8p11: A review. Leukemia 9: 1628-1630, 1995.
2. Fioretos T, Panagopoulos I, Lassen C, Swedin A, Billström R, Isaksson M, Strömbeck B, Olofsson T, Mitelman F and Johansson B: Fusion of the BCR and the fibroblast growth factor receptor-1 (FGFR1) genes as a result of t(8;22)(p11;q11) in a myeloproliferative disorder: The first fusion gene involving BCR but not ABL. Genes Chromosomes Cancer 32: 302-310, 2001.
3. Jackson CC, Medeiros LJ and Miranda RN: 8p11 myeloproliferative syndrome: A review. Hum Pathol 41: 461-476, 2010.
4. Li T, Zhang G, Zhang X, Lin H and Liu Q: The 8p11 myeloproliferative syndrome: Genotypic and phenotypic classification and targeted therapy. Front Oncol 12: 1015792, 2022.
5. Arber DA, Orazi A, Hasserjian R, Thiele J, Borowitz MJ, Le Beau MM, Bloomfield CD, Cazzola M and Vardiman JW: The 2016 revision to the World Health Organization classification of myeloid neoplasms and acute leukemia. Blood 127: 2391-2405, 2016.
6. Abruzzo LV, Jaffe ES, Cotelingam JD, Whang-Peng J, Del Duca V Jr and Medeiros LJ: T-cell lymphoblastic lymphoma with eosinophilia associated with subsequent myeloid malignancy. Am J Surg Pathol 16: 236-245, 1992.
7. Katoh M and Nakagama H: FGF receptors: Cancer biology and therapeutics. Med Res Rev 34: 280-300, 2014.
8. Zhang CL, Tang GS, Guo MQ, Cheng H, Liu MD, Yang JM and Gong SL: Clinical significance of FGFR1 gene abnormalities in blood tumors. Zhongguo Shi Yan Xue Ye Xue Za Zhi 28: 983-988, 2020 (In Chinese).
9. Grand EK, Grand FH, Chase AJ, Ross FM, Corcoran MM, Oscier DG and Cross NC: Identification of a novel gene, FGFR1OP2, fused to FGFR1 in 8p11 myeloproliferative syndrome. Genes Chromosomes Cancer 40: 78-83, 2004.
10. Zhou F, Chen S, Chao H, Zhang R, Zhou M and Pan J: Clinical and gene involved of one case of 8p11 myeloproliferative syndrome with ins(13;8)(q12;p11p23). Zhonghua Xue Ye Xue Za Zhi 36: 291-296, 2015 (In Chinese).
11. Tiong KH, Mah LY and Leong CO: Functional roles of fibroblast growth factor receptors (FGFRs) signaling in human cancers. Apoptosis 8: 1447-1468, 2013.
12. Gallo LH, Nelson KN, Meyer AN and Donoghue DJ: Functions of fibroblast growth factor receptors in cancer defined by novel translocations and mutations. Cytokine Growth Factor Rev 26: 425-449, 2015.
13. Greulich H and Pollock PM: Targeting mutant fibroblast growth factor receptors in cancer. Trends Mol Med 17: 283-292, 2011.
14. Kasyapa CS, Kunapuli P, Hawthorn L and Cowell JK: Induction of the plasminogen activator inhibitor-2 in cells expressing the ZNF198/FGFR1 fusion kinase that is involved in atypical myeloproliferative disease. Blood 107: 3693-3699, 2006.
15. Urrea Pineda LY, Perilla O, Santiago-Pacheco V and Trujillo Montoya S: Myeloproliferative syndrome with eosinophilia associated with translocation t(8; 13) and T-cell lymphoblastic lymphoma: A case report and review of the literature. Cureus 14: e22734, 2022.
16. Buijs A, van Wijnen M, van den Blink D, van Gijn M and Klein SK: A ZMYM2-FGFR1 8p11 myeloproliferative neoplasm with a novel nonsense RUNX1 mutation and tumor lysis upon imatinib treatment. Cancer Genet 206: 140-144, 2013.
17. Chen J, Deangelo DJ, Kutok JL, Williams IR, Lee BH, Wadleigh M, Duclos N, Cohen S, Adelsperger J, Okabe R, *et al*: PKC412 inhibits the zinc finger 198-fibroblast growth factor receptor 1 fusion tyrosine kinase and is active in treatment of stem cell myeloproliferative disorder. Proc Natl Acad Sci USA 101: 14479-14484, 2004.

18. Vizmanos JL, Hernández R, Vidal MJ, Larráyoz MJ, Odero MD, Marı́n J, Ardanaz MT, Calasanz MJ and Cross NC: Clinical variability of patients with the t(6;8)(q27;p12) and FGFR1OP-FGFR1 fusion: Two further cases. Hematol J 5: 534-537, 2004.
19. Popovici C, Zhang B, Gŕegoire MJ, Jonveaux P, Lafage-Pochitaloff M, Birnbaum D and Pébusque MJ: The t(6;8)(q27;p11) translocation in a stem cell myeloproliferative disorder fuses a novel gene, FOP, to fibroblast growth factor receptor 1. Blood 93: 1381-1389, 1999.
20. Guasch G, Mack GJ, Popovici C, Dastugue N, Birnbaum D, Rattner JB and Pébusque MJ: FGFR1 is fused to the centrosome-associated protein CEP110 in the 8p12 stem cell myeloproliferative disorder with t(8;9)(p12;q33). Blood 95: 1788-1796, 2000.
21. Chen MY, Shen HJ, Chao HY, Wang Q, Zhang XW, He C, Cen JN, Chen SN, Zhang R and Zhu MQ: 8p11 myeloproliferative syndrome with CEP110-FGFR1 fusion in a child. Zhonghua Er Ke Za Zhi 57: 297-300, 2019 (In Chinese).
22. Mugneret F, Chaffanet M, Maynadié M, Guasch G, Favre B, Casasnovas O, Birnbaum D and Pébusque MJ: The 8p12 myeloproliferative disorder. t(8;19)(p12;q13.3): A novel translocation involving the FGFR1 gene. Br J Haematol 111: 647-649, 2000.
23. Manur R, Sung PJ, Loren AW, Ritchie EK, Frank D, Bagg A, Geyer JT and Bogusz AM: Leukemic lineage switch in a t(8;22)(p11.2;q11.2)/BCR-FGFR1-rearranged myeloid/lymphoid neoplasm with RUNX1 mutation-diagnostic pitfalls and clinical management including FGFR1 inhibitor pemigatinib. Leuk Lymphoma 61: 450-454, 2020.
24. Khodadoust MS, Luo B, Medeiros BC, Johnson RC, Ewalt MD, Schalkwyk AS, Bangs CD, Cherry AM, Arai S, Arber DA, *et al*: Clinical activity of ponatinib in a patient with FGFR1-rearranged mixed-phenotype acute leukemia. Leukemia 30: 947-950, 2016.
25. Romana SP, Radford-Weiss I, Ben Abdelali R, Schluth C, Petit A, Dastugue N, Talmant P, Bilhou-Nabera C, Mugneret F, Lafage-Pochitaloff M, *et al*: NUP98 rearrangements in hematopoietic malignancies: A study of the groupe francophone de cytogénétique hématologique. Leukemia 20: 696-706, 2006.
26. Onozawa M, Ohmura K, Ibata M, Iwasaki J, Okada K, Kasahara I, Yamaguchi K, Kubota K, Fujisawa S, Shigematsu A, *et al*: The 8p11 myeloproliferative syndrome owing to rare FGFR1OP2-FGFR1 fusion. Eur J Haematol 86: 347-349, 2011.
27. Belloni E, Trubia M, Gasparini P, Micucci C, Tapinassi C, Confalonieri S, Nuciforo P, Martino B, Lo-Coco F, Pelicci PG and Di Fiore PP: 8p11 myeloproliferative syndrome with a novel t(7;8) translocation leading to fusion of the FGFR1 and TIF1 genes. Genes Chromosomes Cancer 42: 320-325, 2005.
28. Walz C, Chase A, Schoch C, Weisser A, Schlegel F, Hochhaus A, Fuchs R, Schmitt-Gräff A, Hehlmann R, Cross NC and Reiter A: The t(8;17)(p11;q23) in the 8p11 myeloproliferative syndrome fuses MYO18A to FGFR1. Leukemia 19: 1005-1009, 2005.
29. Hidalgo-Curtis C, Chase A, Drachenberg M, Roberts MW, Finkelstein JZ, Mould S, Oscier D, Cross NC and Grand FH: The t(1;9)(p34;q34) and t(8;12)(p11;q15) fuse pre-mRNA processing proteins SFPQ (PSF) and CPSF6 to ABL and FGFR1. Genes Chromosomes Cancer 47: 379-385, 2008.
30. Soler G, Nusbaum S, Varet B, Macintyre EA, Vekemans M, Romana SP and Radford-Weiss I: LRRFIP1, a new FGFR1 partner gene associated with 8p11 myeloproliferative syndrome. Leukemia 23: 1359-1361, 2009.
31. Wasag B, Lierman E, Meeus P, Cools J and Vandenberghe P: The kinase inhibitor TKI258 is active against the novel CUX1-FGFR1 fusion detected in a patient with T-lymphoblastic leukemia/lymphoma and t(7;8)(q22;p11). Haematologica 96: 922-926, 2011.
32. Kim SY, Kim JE, Park S and Kim HK: Molecular identification of a TPR-FGFR1 fusion transcript in an adult with myeloproliferative neoplasm, T-lymphoblastic lymphoma, and a t(1;8)(q25;p11.2). Cancer Genet 207: 258-262, 2014.
33. Gervais C, Dano L, Perrusson N, Hélias C, Jeandidier E, Galoisy AC, Ittel A, Herbrecht R, Bilger K and Mauvieux L: A translocation t(2;8)(q12;p11) fuses FGFR1 to a novel partner gene, RANBP2/NUP358, in a myeloproliferative/myelodysplastic neoplasm. Leukemia 27: 1186-1188, 2013.
34. Nakamura Y, Ito Y, Wakimoto N, Kakegawa E, Uchida Y and Bessho M: A novel fusion of SQSTM1 and FGFR1 in a patient with acute myelomonocytic leukemia with t(5;8)(q35;p11) translocation. Blood Cancer J 4: e265, 2014.
35. Wang T, Wang Z, Zhang L, Wen L, Cai W, Yang X, Pan J, Ruan C, Wu D, Sun A and Chen S: Identification of a novel TFG-FGFR1 fusion gene in an acute myeloid leukaemia patient with t(3;8)(q12;p11). Br J Haematol 188: 177-181, 2020.
36. Zhang X, Wang F, Yan F, Huang D, Wang H, Gao B, Gao Y, Hou Z, Lou J, Li W and Yan J: Identification of a novel HOOK3-FGFR1 fusion gene involved in activation of the NF-kappaB pathway. Cancer Cell Int 22: 40, 2022.
37. Liu PCC, Koblish H, Wu L, Bowman K, Diamond S, DiMatteo D, Zhang Y, Hansbury M, Rupar M, Wen X, *et al*: INCB054828 (pemigatinib), a potent and selective inhibitor of fibroblast growth factor receptors 1, 2, and 3, displays activity against genetically defined tumor models. PLoS One 15: e0231877, 2020.
38. Kalyukina M, Yosaatmadja Y, Middleditch MJ, Patterson AV, Smaill JB and Squire CJ: TAS-120 cancer target binding: Defining reactivity and revealing the first fibroblast growth factor receptor 1 (FGFR1) irreversible structure. ChemMedChem 14: 494-500, 2019.
39. Hu T, Wu Q, Chong Y, Qin H, Poole CJ, van Riggelen J, Ren M and Cowell JK: FGFR1 fusion kinase regulation of MYC expression drives development of stem cell leukemia/lymphoma syndrome. Leukemia 32: 2363-2373, 2018.
40. Xu LP, Chen Y, Shi HX and Huang XJ: 8p11 myeloproliferative syndrome cured by allogeneic hematopoietic stem cell transplantation: Two case reports and literature review. Beijing Da Xue Xue Bao Yi Xue Ban 45: 993-996, 2013 (In Chinese).
41. Larosa F, Maddens S, Legrand F, Pouthier F, Ferrand C, Saas P, Hayette S, Chabod J, Tiberghien P, Rohrlich PS and Deconinck E: Early immune reconstitution and efficient graft vs tumor effect after unrelated partially matched double cord blood transplantation in refractory 8p11 syndrome. Bone Marrow Transplant 46: 622-624, 2011.